Dynamic Model-Based Safety Margins for High-Density Matrix Headlight Systems

Jens Schleusner, Holger Blume, *Senior Member, IEEE,* and Sebastian Lampe

***Abstract*—Real-time masking of vehicles in a dynamic road environment is a demanding task for adaptive driving beam systems of modern headlights. Next-generation high-density matrix headlights enable precise, high-resolution projections, while advanced driver assistance systems enable detection and tracking of objects with high update rates and low-latency estimation of the pose of the ego-vehicle. Accurate motion tracking and precise coverage of the masked vehicles are necessary to avoid glare while maintaining a high light throughput for good visibility. Safety margins are added around the mask to mitigate glare and flicker caused by the update rate and latency of the system. We provide a model to estimate the effects of spatial and temporal sampling on the safety margins for high- and low-density headlight resolutions and different update rates. The vertical motion of the ego-vehicle is simulated based on a dynamic model of a vehicle suspension system to model the impact of the motion-to-photon latency on the mask. Using our model, we evaluate the light throughput of an actual matrix headlight for the relevant corner cases of dynamic masking scenarios depending on pixel density, update rate, and system latency. We apply the masks provided by our model to a high beam light distribution to calculate the loss of luminous flux and compare the results to a light throughput approximation technique from the literature.**

***Index Terms*—Matrix Headlights, Real-time Masking, Motion-to-Photon Latency, Light Throughput**

I. Introduction

HEADLIGHTS are an important safety component of every vehicle as they are critical for good visibility while driving at night. Traditional headlights provide a bright high beam to illuminate the area ahead and a low beam that only lights up the area below the headlight's horizon to avoid glaring oncoming traffic. Improved visibility has been achieved by the development of brighter high beams based on Xenon, LED, or even Laser light sources for ranges up to 600 m [1]. It is important to avoid glare for other road users by selecting low beams when driving towards other traffic as glare by high beams causes strong discomfort and even short-term blindness to objects in the dark. A study shows that the perceived discomfort and the re-adaptation time of the eye increase significantly when the glare exposure is longer than 300 ms [2]. A different study shows that eyes that were exposed to headlights need at least 1 s to recover and even more time when exposed to higher luminance or longer exposure times [3].

Manuscript received 19 September 2022; revised 24 February 2023; accepted 03 March 2023

J. Schleusner and H. Blume are with the Institute of Microelectronic Systems, Leibniz University Hannover, 30167 Hannover, Germany e-mail: {jens.schleusner, holger.blume}@ims.uni-hannover.de

S. Lampe is with Volkswagen AG, Exterior Lighting Systems, 38436 Wolfsburg, Germany, e-mail: sebastian.lampe@volkswagen.de

Technologies to automatically switch from high beams to low beams by optically detecting oncoming traffic have been developed as early as 1958 [4]. Modern vehicles are equipped with cameras, RADAR, LiDAR, and other sensors to detect traffic, pedestrians, and features of the environment for assistive functions and safety features like automatic emergency braking and lane-departure warnings. These Advanced Driver Assistance Systems (ADAS) can supply information about the environment and other road users that are potentially within the beam of the headlights. These data can be used to automatically switch between low beam and high beam depending on the current traffic conditions. Specific light functions for different environments like highway mode, city light, and offroad modes can be activated as well.

Only deciding between static low and high beam light distributions is inefficient on roads with high traffic as there are often drivers within the headlights field of view (FOV) that could be exposed to glare. To maximize the brightness and visibility for the driver while minimizing glare for others in the illuminated area, adaptive driving beam (ADB) matrix systems with multiple individually controllable emitters per headlight are used [5]. The high beam light distribution can be disabled in specific regions of oncoming traffic to avoid glare while maintaining a high light throughput. The masks to avoid glare are supplied by improved ADAS sensors, which generate precise 3D data about the current driving scenario [6]. Technological advances such as LED-matrix-, LCD- or Digital Micromirror Device (DMD)-Headlights allow increased resolutions and increase the emitter density of these matrix lights from a few individual lamps to thousands or millions of pixels [7]. We focus on next-generation systems with more than 1000 light emitters in a 2D matrix of multiple rows and columns, as these higher resolution pixel headlights enable new applications like the precise masking of small objects such as reflective signs, pedestrians, and cyclists [8]. Maximizing light throughput without causing glare is the primary optimization goal in matrix headlight design. In this paper, we describe the effects that affect light throughput in dynamic masking scenarios and model them as spatial and temporal sampling processes. Higher pixel density improves the masking accuracy and therefore reduces the spatial sampling loss. The temporal sampling process models the effect of updating masks at a discrete update rate. Therefore, commercial systems require safety margins around the masks [7] to compensate for the dynamic motion of the masked object during update cycles to achieve continuous masking. We use our model to evaluate the loss of light throughput due to different pixel densities and update rates. Moreover, we introduce a model to evaluate

 DOI: https://doi.org/10.1109/TITS.2023.3264768

TABLE I
SELECTED TECHNOLOGIES FROM THE LITERATURE THAT REPRESENT THEIR RESPECTIVE CATEGORY OF PIXEL DENSITY IN OUR EVALUATION.

Category	Technology	Resolution	FOV	Density $D = f^{-1}$	
		px	°	°/px	mm/px
Matrix	LED [10]	128x32	32x8	0.25	4.5
HD-Matrix	LCD [11]	300x100	30x10	0.1	1.8
DMD	DMD [12]	1152x576	15x8	0.01	0.2

glare caused by the headlight's up and down motion due to a vertical ego-motion of the vehicle. The effect of the motion on the masks can be corrected in a Headlight Leveling System (HLS) based on data from motion sensors [9]. Additional vertical safety margins are applied to compensate for the latency of the sensor system. Current systems have latencies of several hundred milliseconds [9] as they are based on traditional vehicle architectures that were designed without low latency data paths for the headlight systems. Using our model, we show that these architectures with latencies above 100 ms require safety margins that disable entire pixel columns to reliably compensate for vertical ego-motion.

The remainder of this paper is organized as follows. Section II covers existing technologies, parameters, and metrics. Sections III to V introduce our spatial- and temporal sampling and ego-motion models. We evaluate the light throughput based on our models in section VI and conclude the work in section VII.

II. Related Work

Multiple new applications are enabled by matrix headlights. Arbitrary static light distributions such as high and low beams and adjustments to the low beam pattern for left-hand-driving can be digitally emulated. In addition, dynamic changes to the projection are possible. The light output can be rotated horizontally in curves and raised or lowered vertically to adjust to the oncoming terrain [13]. Mechanical actuators to move the lamp can be eliminated in favor of a solid-state matrix headlight. Furthermore, masks can be overlayed onto the light distribution to avoid glare for oncoming traffic and to reduce the intensity of light reflections towards the driver from reflective objects such as traffic signs [8]. Analogous to masks, the projection of bright spots to highlight features in front of the car such as pedestrians or animals is possible [14]. If the resolution is sufficiently high, texture can be projected onto the road to assist with navigation through construction zones or visualize brake distances with projected guidelines [15]. Manufacturers also developed animated image projections as welcome light or pictographic warning symbols similar to the content shown in a Head-up display (HUD) [15].

A. Headlight Technologies

The industry offers a wide range of matrix headlights to provide spatial and temporal sampling capabilities for ADB functions such as glare-free high beams. The Multi-LED-headlight module with 84 pixels by automotive supplier Hella is commonly used by Mercedes [16], Porsche [17] and others as ADB system. Samsung provides an implementation with

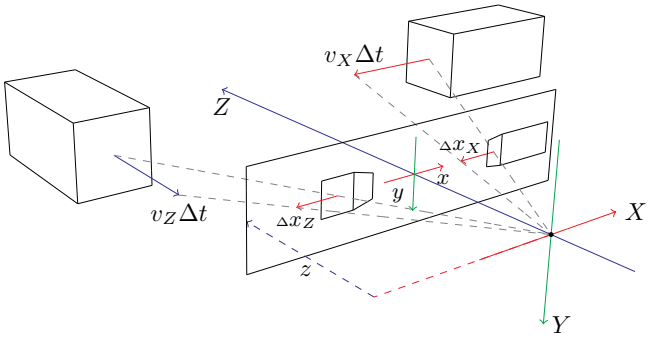

Fig. 1. Vehicles move parallel (blue) and perpendicular (red) to the optical Z-axis of the headlight located at $(X, Y, Z) = (0, 0, 0)$m. Their bounding boxes are projected onto the virtual screen with its coordinate system xy at $Z = 1$ m. The displacement vector $v\Delta t$ models the position change of the object within an update cycle Δt. The displacement vectors for both scenarios are projected to a horizontal shift Δx on the screen as shown by the gray lines.

up to 192 LED pixels on a single emitter [18] and a Japanese research group proposes 288 LEDs per headlight [19]. LED-matrices with higher resolutions of more than 1000 pixels are currently developed by research groups. These LED-Matrix headlights are not based on individual lamps with their own optics but instead consist of a single rectangular LED light divided into a 2D grid of individual pixels called Chip on board (COB), which enables higher resolution, pixel density, and the use of a common projection optic. These next-generation high-resolution matrices are the focus of this research paper. As headlight systems from different manufacturers each have different parameters, we categorize the published case studies based on the provided resolution into Matrix-, high density (HD)-Matrix- and DMD-Headlights.

1) Matrix-Headlights: The micro Adaptive Front lighting System (µAFS) project has developed a Matrix-LED chip with 1024 pixels [10], which is currently in production by Osram [20]. The LED technology can be switched with very low latency, which enables a high update rate of up to 400 Hz for the µAFS system [10]. With a projection optic, it provides a horizontal density of 0.25 °/px. Valeo and CREE propose a LED chip with a pixel count of 4000 px that provides the same vertical resolution with a wider horizontal FOV [21].

2) HD-Matrix-Headlights: Generally, HD-Matrix Headlights have more than 10 000 px, which enables a density of at least 0.1 °/px, which is sufficient to mask even small objects with glare-free-high beams [13]. The next generation of the µAFS LED chip will have a much higher pixel count of 25 600 px [22]. Another implementation by Hella provides 16 000 px on a single emitter [23]. High-density LED matrices are difficult to manufacture due to the high level of integration and require advanced cooling due to their high power densities but have the advantage that LEDs are self-luminous and contribute to the power budget only when they are lit. A different approach to high-resolution headlights is LCD-based systems. Pixel counts of 30 000 px [11] up to 54 000 px [7] have been achieved using LCD panels within the optical path which enable a density of 0.1 °/px. Individual pixels of the LCD panel can be controlled to selectively pass or block

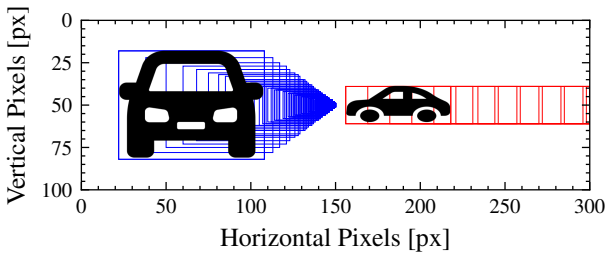

Fig. 2. The figure shows a 200 km/h (56 m/s) parallel (blue, left) and 100 km/h (28 m/s) perpendicular (red, right) scenario relative to the pixel array of a HD-matrix headlight. The vehicle is sampled at 30 Hz and enclosed by a bounding box that can be used to mask a light distribution.

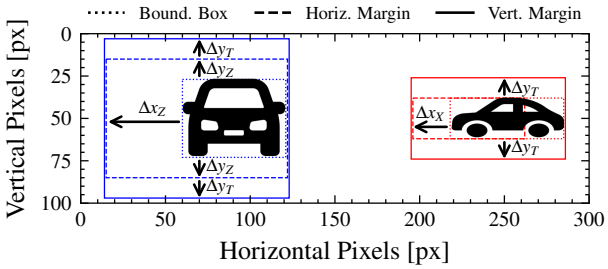

Fig. 3. The plot shows a snapshot of the scenarios presented in Fig. 2. The detected vehicle is enclosed by a pixel-aligned bounding box (spatial sampling). A horizontal safety margin is applied to compensate for temporal sampling and a vertical margin is applied to compensate for the system latency.

the light that is projected onto the road at a rate of 60 Hz [11]. A major disadvantage of this LCD technology compared to LED matrices is that it is a subtractive process with a LED light source that is always on. In addition to the up to 50 % transmission loss of the LCD panel itself, light from the masked areas has to be dissipated within the LCD [24].

3) DMD-Headlights: Another approach is the DMD technology [12]. The LCD is replaced by a Micro-Electro-Mechanical System (MEMS)-based DMD chip. Each pixel on the chip consists of a microscopic silicon mirror that can direct light from the lamp either onto the road or onto an adsorbing material. This technology is more robust compared to LCDs as heat is not dissipated within the sensitive active element. As with LCDs, full power is always required, regardless of the number of lit pixels. DMD headlights are available in very high resolutions of up to 2 megapixels, as the projection technology is already developed and used in digital video projectors. DMD-based headlights are commercially available from Mercedes [15] and Audi [25]. Moreover, they are used in research projects as DMDs can be driven at very low latencies and update rates up to 1 kHz [26]. DMD systems are the only state-of-the-art technology to provide a density of 0.01 °/px in a headlight. TABLE I shows the technologies that are evaluated here.

B. Model Parameters

The headlights of different manufacturers each have different projection parameters as shown in TABLE I. For our evaluation, the resolution of the matrix and the focal length of the optical engine are relevant to model the pixel density. In the headlight community, resolution and pixel density are sometimes used interchangeably [7]. In this paper, the resolution is defined as the matrix size in pixels, while pixel density describes the resolution relative to the environment. The density is typically specified relative to a solid angle in °/px. For the rectangular flat light emitters modeled in this paper, this metric only gives an average approximation to the true parameters of a single pixel. As the evaluation presented in this paper relies on an accurate representation of the properties of these pixels, we specify the density in mm/px for the projection on a vertical projection surface 1 m in front of the headlight, which characterizes the true size of all pixels on that screen [27]. In our evaluation, the pixels are assumed to be square and the lens geometry is assumed to be symmetric. Arbitrary pixel aspect ratios can be specified in our model, but this is not necessary for modeling the uniform matrix emitters selected for the evaluation. Therefore, in this paper, the pixel density is the same in the x and y directions and is specified as a single parameter D. The mathematical model uses the focal length $f = D^{-1}$ from the pinhole camera model specified in px/m at a distance of 1 m [27], which is equal to the inverse of the pixel density D specified in m/px.

C. ADB- and Headlight Leveling Systems

Data on the vehicle state relative to the environment is provided by multiple sensors. An inertial measurement unit (IMU) provides data on the vehicle's ego-movement and cameras or LIDAR detect and localize other road users. These data are fused by a processing unit and provided to the ADB-system [6] and the HLS [28] to generate the light patterns and masks, which are then transferred to the headlights and projected onto the road. Every step of the data processing pipeline from the sensors to the headlights has a specific delay, which can be accumulated to the total system latency. From a rendering perspective, the latency requirements of a pixel headlight system are similar to modern Augmented Reality (AR) devices. The key challenge that separates these devices from many other video processing applications is the direct interaction of the rendered content with the dynamic environment in real-time [29]. System latency is the most important parameter of a real-time processing architecture for a modern headlight. For our evaluation, two latency paths through the system are relevant. The delay between the recording of a vehicle bounding box and the adaptation of the headlight mask is called *adaptation time* [5]. In the US, SAE-J3069 [30] requires an adaptation time of 2.5 s for the initial response to a vehicle followed by continuous masking. A study by the NHTSA [5] shows, that the average adaptation time of current commercial ADB systems lies between 560 ms (Audi A8) and 1.2 s (BMW X5). In research implementations, latencies as low as 2.5 ms are possible [26]. The latency between an IMU and the headlight in a HLS is called *Motion-to-Photon Latency* [29]. A study by the UNECE Working Party on Lighting and Light-Signaling [9] measured average latencies of 100 ms (Audi A3), 350 ms (Opel Insignia) and 500 ms (Audi S3). In their proposal to UNECE-R48 [31], the authors

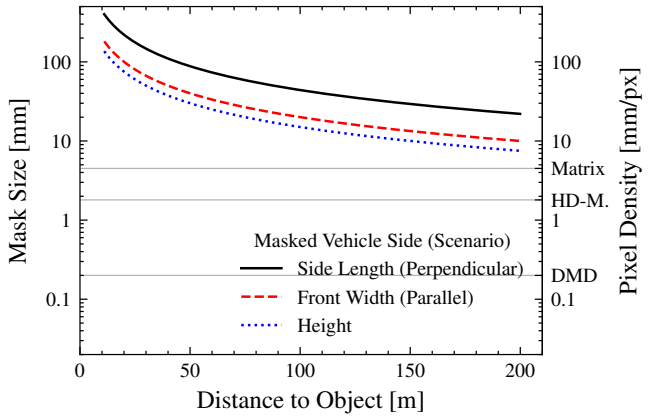

Fig. 4. The size of the mask on the virtual projection screen 1 m in front of the headlight depends on the distance to the masked vehicle and the pixel density of the headlight. The mask height is orientation independent. In perpendicular scenarios, the mask width covers the vehicle length, in parallel scenarios the vehicle width. To mask a compact car as assumed in this plot, multiple pixels are disabled by the mask.

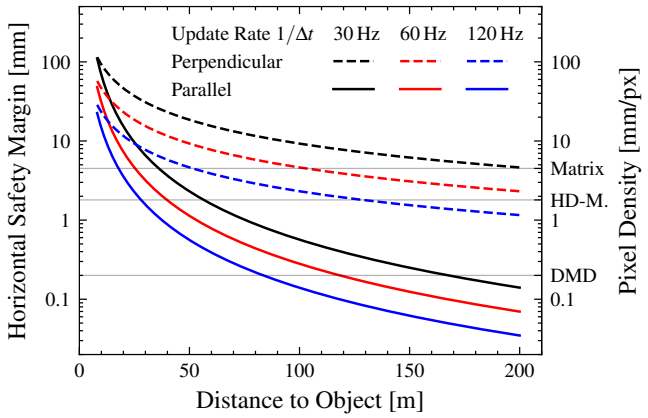

Fig. 5. These graphs show the size of the required horizontal safety margin for a mask tracking a vehicle in a 200 km/h (56 m/s) parallel and 100 km/h (28 m/s) perpendicular scenario. The masked vehicle is in view for distances above 10 m. For each new frame displayed by the headlight, the mask is shifted horizontally to overlap the vehicle. To mitigate glare between these shifts, a safety margin has to be applied to the mask to compensate this shift in advance.

suggest a reaction time of 220 ms to 350 ms for dynamic leveling of low beams. In addition to these requirements, the continuous masking is individually evaluated for compliance with UNECE-R48. Commercial systems are classified either as ADB systems, which often reduce the adaptation time by improving temporal sampling with higher update rates [10] or as HLS, which reduce the system latency to improve the dynamic reaction time [6]. We model the impact of both effects on the resulting light throughput and provide a model to evaluate the combined effects in dynamic scenarios to achieve continuous masking. The impact of the adaptation time is modeled in section IV and the evaluation based on the motion-to-photon latency is presented in section V.

III. Spatial Sampling Model

A projective transformation maps every 3D point $(X, Y, Z)^\intercal$ of the environment within the illuminated image cone of the headlight to a 2D coordinate $(x, y)^\intercal$ in the virtual image plane. The mapping uses a pinhole camera model with focal length f in a camera coordinate system relative to the optical center of the headlight [27]. The projective transformation according to Eq. 1 is shown in Fig. 1.

$$\begin{pmatrix} x \\ y \end{pmatrix} = f \frac{z}{Z} \begin{pmatrix} X \\ Y \end{pmatrix} \tag{1}$$

To mask a 3D object such as an oncoming vehicle, the contour of the object is transformed into a 2D bounding box on the virtual image plane at $z = 1\,\mathrm{m}$ in front of the headlight according to Eq. 1. Fig. 4 shows the size of the bounding box in the image plane for a compact car of 4.4 m length by 2.0 m width by 1.5 m height positioned at varying distances. The projected bounding box is used as an anti-glare mask for the headlight projection. The required mask size varies depending on whether the vehicle is traveling perpendicular or parallel to the headlight's optical Z-axis. The mask height remains constant for both orientations, while the mask width changes depending on whether the front or the side of the vehicle is masked. In the coordinate system of the image plane, the mask size can be directly compared to the headlight pixel density $D = f^{-1}$ to evaluate the relative scale of the mask compared to the headlight pixels. In the image plane, the 2D bounding box of the vehicle is spatially sampled to the discrete pixel grid of the headlight. This is modeled by expanding the bounding box to integer multiples of the pixel size to prevent glare or strobe effects at the mask edges. Fig. 4 shows that for the systems, objects, and distances evaluated here, the pixel size is at least $2\times$ smaller than the masked object. For smaller objects or lower pixel densities, a saturation of the mask size to a minimal length and width of 1 px will occur. The rendered masks are based on the object positions provided by the sensor system. Assuming sufficient localization precision, this sampling model can achieve perfect masking for static objects that are not moving relative to the vehicle. In section IV, this model is extended to moving objects.

IV. Temporal Sampling Model

We model the masking of moving objects as a temporal sampling process. In addition to the static spatial sampling model presented in the previous section, the sampling time Δt in ms must be taken into account. Here, the sampling time is the inverse of the update rate of the headlight.

A. Sensor Fusion and Prediction

Object positions and bounding boxes are usually not available in real-time at the framerate of the rendering system of a pixel headlight. Moreover, inherent system latencies due to acquisition delays, processing, and transmission of the information further delay the masking relative to the masked movement. As objects move predictably at a constant velocity on this millisecond timescale, a tracking algorithm can be used to predict intermediate data for the object location at the rendering time of the frames to compensate for the latencies and render the correct masks for the object positions during the light output [32].

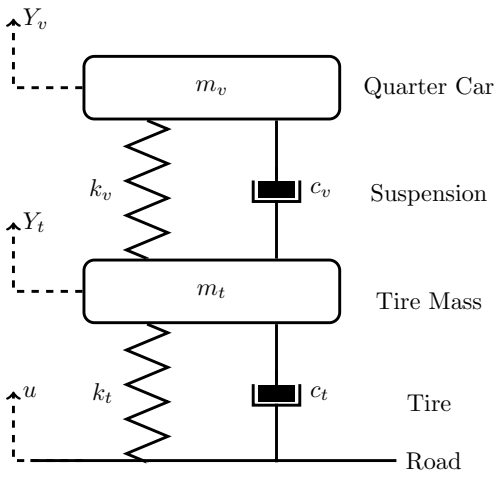

Fig. 6. A quarter-car model is used to simulate the vertical dynamics (ego-motion) of the own vehicle based on the step response of a tire and suspension system. The differential equation model takes mass, spring stiffness, and damping coefficients into account.

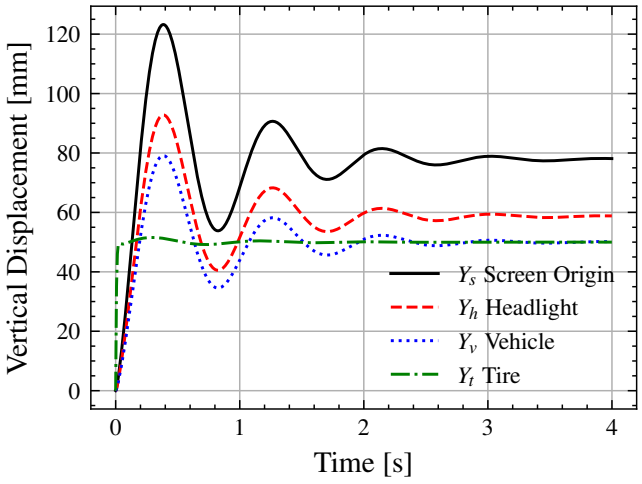

Fig. 7. The 50 mm step response for a tire and a vehicle is simulated based on the quarter car model and used to calculate the vertical displacement of the headlight and the virtual screen origin.

B. Safety Margins

To steadily mask the 3D points of an object's bounding box that moves relative to the headlight, the corresponding disabled pixels given by the spatial sampling model are shifted at each frame update, as shown in Fig. 2. Large distances to the object require only minor corrections. Objects at an infinite distance always correspond to the same pixel that represents the vanishing point. The closer a moving object is, the larger the shift difference required for each frame. If the shift per frame is higher than the pixel density of the headlight, glare can occur if the object moves outside its mask before the mask is corrected in an updated frame. To avoid glare, the mask must be extended by a safety margin as shown in Fig. 3. This safety margin is applied only in the direction of the pixel's motion to keep as much light unmasked as possible. Fig. 3 shows the required horizontal safety margin on a virtual projection surface at $z = 1\,\mathrm{m}$ in front of the vehicle to track parallel and perpendicular traveling vehicles with a mask. The size of the safety margin is determined by the shift per frame between the current mask and the next mask to ensure continuous masking between rendering updates.

C. Dynamic Masking Model

In a dynamic road environment, the 3D coordinates of each point change with time t. Therefore, the static spatial sampling model described by Eq. 1 is extended to a temporal sampling model in Eq. 2, which maps arbitrary time-variant object trajectories to their corresponding image coordinates.

$$\begin{pmatrix} x(t) \\ y(t) \end{pmatrix} = f \frac{z}{Z(t)} \begin{pmatrix} X(t) \\ Y(t) \end{pmatrix} \tag{2}$$

The headlight must adapt the masks to this motion at a discrete sample rate with interval Δt. During the update interval, the object is translated by a 3D-displacement vector $\Delta(X, Y, Z)^\intercal = v\Delta t$, which is projected onto the image plane as a shift per frame $\Delta(x, y)^\intercal$ (see Fig. 1). This shift corresponds to the safety margin required to keep the object masked during the update interval. The geometric intersection of masks transformed by Eq. 2 at successive timestamps approximates the safety margins for arbitrary motion scenarios. Object trajectories relevant for this evaluation occur in the road-parallel XZ-plane of the headlight coordinate system. Therefore, scenarios are constructed from a parallel and a perpendicular motion component relative to the optical Z-axis. The shift Δx for both corner cases is visualized in Fig. 3 and modeled in the following sections.

D. Perpendicular Masking Model

Perpendicular moving objects such as crossing traffic at an intersection are characterized by a constant distance Z to the headlight at a constant height Y. This results in a constant height y of the corresponding headlight pixel. Therefore, perpendicular movement can be modeled by only taking the X-axis into account. For a vehicle driving at speed v_x, the relative change Δx of the horizontal pixel position within a frame update cycle Δt is derived from Eq. 2:

$$\Delta x = fz\frac{1}{Z}\Delta X = fz\frac{1}{Z}v_x\Delta t \tag{3}$$

The calculated shift per frame is used as a horizontal safety margin to expand the bounding box. For a perpendicular movement with a speed of 100 km/h at different distances, Fig. 5 shows the horizontal shift per frame projected into the image plane. The crossing of the pixel density D characterizes a horizontal shift of 1 px which limits the best masking precision for a given technology. With this model, an upper limit for the update interval Δt_{max} can be derived to achieve a 1 px masking precision at a given distance Z.

$$\Delta t_{max} = \frac{1}{fzv_x}\Delta x Z \tag{4}$$

For a given headlight, the distance at which perfect masking is possible can be decreased significantly with higher update rates. Fig. 5 shows that in this case, masking of perpendicular

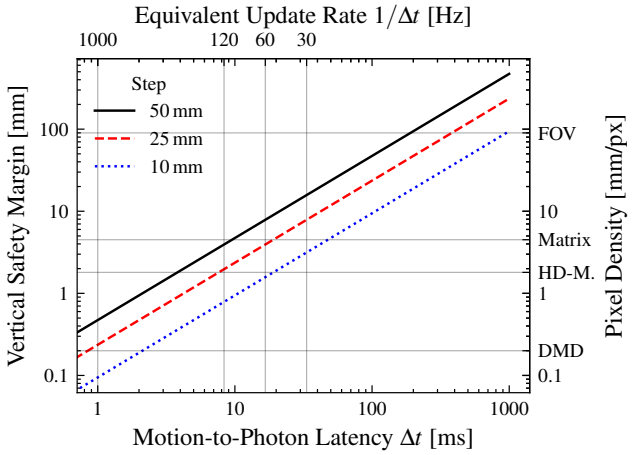

Fig. 8. The vertical safety margin derived from the step response is proportional to the motion-to-photon latency. If the safety margin extends above the FOV (±5°), the mask covers the full vertical resolution of the headlight. For a single-pixel safety margin, the motion-to-photon latency must be reduced below the crossing of the pixel density of the headlight.

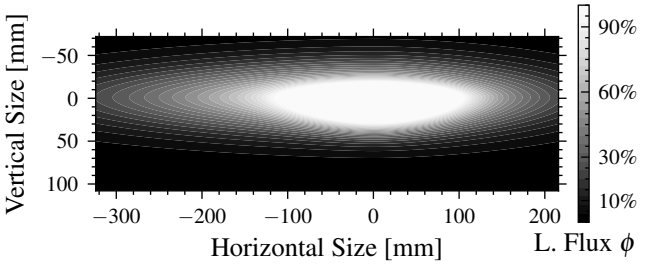

Fig. 9. This figure shows the light distribution of the high beam of a left headlight in the virtual screen coordinate system introduced in Fig. 1. It has the maximum luminous flux along the optical center axis. The luminous flux of this left headlight is distributed asymmetrically and extends further to the left.

traveling vehicles with minimal safety margins is possible for LED-matrix resolutions at 60 Hz above 100 m and for HD-matrix resolutions at 120 Hz above 120 m. Headlights with a higher resolution of the DMD technology must apply multi-pixel safety margins or significantly higher update rates to avoid glare.

E. Parallel Masking Model

The parallel scenario describes that the vehicle is driving on a straight road along the Z-axis with an object to be masked located at distance Z with offset $(X, Y)^\intercal$. With Eq. 2, the relative change of the pixel position $(\Delta x, \Delta y)^\intercal$ within a frame delay Δt can be derived for an object driving at relative speed v_z:

$$\begin{pmatrix}\Delta x\\ \Delta y\end{pmatrix} = fz\left(\frac{1}{Z} - \frac{1}{Z - v_z\Delta t}\right)\begin{pmatrix}X\\ Y\end{pmatrix} \tag{5}$$

In this parallel case, the horizontal shift Δx dominates the vertical shift Δy. Except for overhead signage, most objects and vehicles to be masked are approximately within the XZ-plane of the headlight. Fig. 5 shows the horizontal shift per frame for the parallel case of two cars at 100 km/h approaching each other. Compared to the perpendicular scenario, the horizontal shift in the image plane is much smaller because the motion vector is parallel to the optical axis. An upper limit of the update interval Δt_{max} for pixel-precise masking can be derived:

$$\Delta t_{max} = \frac{\Delta x Z^2}{fzv_zX - \Delta x v_z Z} \tag{6}$$

A DMD headlight can achieve pixel-precise masking below 85 m with a refresh rate of 120 Hz. A HD-matrix headlight can achieve this at 40 m at 60 Hz due to its lower pixel density.

V. Ego-Motion Masking Model

In addition to the relative movement of the road objects in the XZ-plane of the headlight, the up and down motion of the headlight along the Y-axis due to vertical vehicle dynamics must be considered as a constraint for the height of the safety margin of the masks. In contrast to the motion of the masked objects along the road, the immediate displacement due to faults in the road surface is not predictable. Therefore, the actual motion-to-photon latency has to be taken into account for the ego-motion model instead of the more relaxed constraint on the projection update rate for predictable movements. In research, road bumps are used as a corner case for vertical vehicle dynamics as they are modeled with a step response when crossed by a vehicle [28]. The vertical vehicle motion is modeled by a system of differential equations. For the example calculations in this paper, we selected the step response of a quarter-car as the basis of our model to approximate the complex suspension model of a commercial HLS [28]. It describes a quarter of a vehicle consisting of a single tire and its suspension system [33] as shown in Fig. 6. Using the transfer function of the system [34] and the specific vehicle parameters like mass of the quarter car m_v and tire mass m_t, spring stiffness k and damping coefficients c, the tire step response $Y_t(t)$ can be computed for a given step u in the road profile. We selected the following values for the compact car evaluated here:

$$\begin{aligned} m_v &= 300\,\text{kg} & k_v &= 17.2\,\text{kN/m} & c_v &= 1.0\,\text{kN s/m}\\ m_t &= 15\,\text{kg} & k_t &= 191\,\text{kN/m} & c_t &= 2.5\,\text{kN s/m}\end{aligned}$$

The response of the vehicle $Y_v(t)$ can be derived from these parameters as well.

$$m_v\ddot{Y_v} = k_v(Y_t - Y_v) + c_v(\dot{Y_t} - \dot{Y_v}) \tag{7}$$

$$m_t\ddot{Y_t} = k_t(u - Y_t) \quad + c_t(\dot{u} - \dot{Y_t}) - m_v\ddot{Y_v} \tag{8}$$

Fig. 7 shows this step response Y_t and Y_v for the tire and the vehicle chassis displacement for a step of 50 mm. From the vertical displacement Y_v of the assumed stiff vehicle chassis, an equation for the displacement Y_h of the headlight can be derived using the wheelbase w (2.6 m) and the X-offset of the headlight X_h (0.5 m) in front of the front axis. Furthermore, the vertical shift Y_s of the image screen origin ($z = 1$ m) can be computed. The tire is very stiff and closely follows the step in the road profile whereas the vehicle chassis and the mounted headlight swing on the suspension system.

$$Y_h = \frac{Y_v}{w}(w + X_h) \qquad Y_s = \frac{Y_v}{w}(w + X_h + z) \tag{9}$$

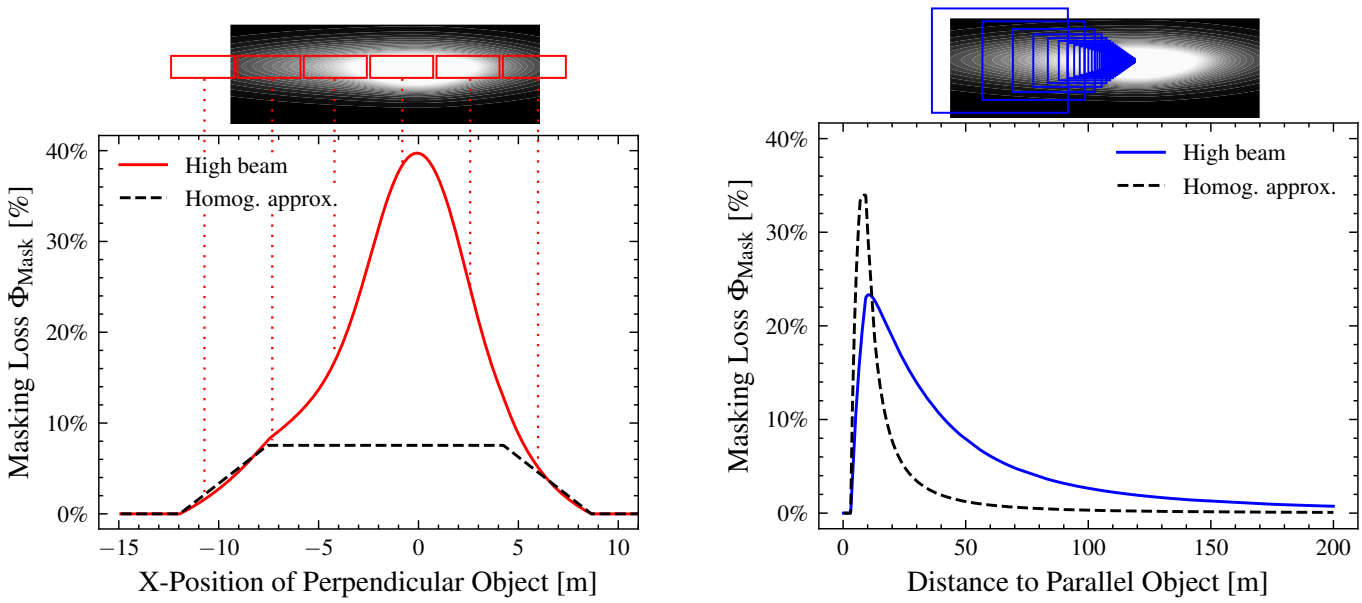

(a) Perpendicular masking loss

(b) Parallel masking loss

Fig. 10. The diagrams show the luminous flux lost by masking a high beam distribution. In the perpendicular scenario, a vehicle crosses the field of view at a 30 m distance. We plotted the mask relative to the light distribution and the corresponding masking loss on the same X-axis. The homogeneous approximation assumes that the luminous flux is uniformly distributed over all pixels, resulting in a loss proportional to the mask size. This approximation underestimates the masking loss, especially near the center point where the actual masking loss is four times higher than the approximated one. In the parallel scenario, the mask crosses the FOV at a distance of 10 m. At shorter distances, the approximation overestimates the masking loss; above this point, it underestimates it.

With a given motion-to-photon latency Δt, the vertical shift per frame Δy can be computed for the headlight.

$$\Delta y(t) = Y_s(t) - Y_s(t - \Delta t) \tag{10}$$

Fig. 8 shows the vertical shift per frame for multiple motion-to-photon system latencies based on the maximum vertical shift of the step response shown in Fig. 7. For this vehicle and tire-suspension configuration and a step of 50 mm, a latency of less than 9 ms is required for minimal safety margins with LED-matrix headlights. If the headlight latency is determined by the update interval, this would correspond to a 120 Hz update rate. Headlights with higher resolution require even lower latencies or taller safety margins. At HD-matrix resolution, a motion-to-photon latency of 3 ms is required. For latencies above 200 ms, the vertical safety margin required to compensate for a step of 50 mm covers the entire vertical FOV ($\pm 5°$) of the headlight.

VI. Light Throughput Evaluation

A headlight system must provide as much light as possible for the driver without causing glare for other road users to maximize road safety. Especially when masking the light distribution, it is important to keep as much of the scene illuminated to keep the object visible to the driver and enable the driver to react accordingly. The authors of [26] and [35] introduce *Light Throughput* as an evaluation metric for different headlight masking strategies. They define it as the percentage of projector pixels per frame that remains on while masking an object of a given size. The authors propose a custom-built video projector-based DMD headlight that provides a homogeneous light distribution to evaluate the light throughput for a parallel scenario and different latencies. In an actual headlight, the light distribution is inhomogeneous, as it is brightest in the center and dimmer towards the sides to maximize visibility, comply with regulations and stay within the limited available power budget [31]. We take this inhomogeneity into account when calculating the masking loss Φ_{Mask} by weighting the n masked pixels according to the relative luminous flux ϕ_i specified by a high beam light distribution as shown in Fig. 9.

$$\Phi_{\text{Mask}} = \sum_{i}^{n} \phi_i \tag{11}$$

The light throughput Φ for a time point depends on the masking loss Φ_{Mask} that is caused by disabling the light distribution within the vehicle bounding box and the loss caused by three additional safety margins: spatial sampling loss Φ_{SS}, temporal sampling loss Φ_{TS}, and ego-motion loss Φ_{EM}. Using our masking models, we investigate the impact of the components on the light throughput separately.

$$\Phi = 1 - \Phi_{\text{Mask}} - \Phi_{\text{SS}} - \Phi_{\text{TS}} - \Phi_{\text{EM}} \tag{12}$$

In our evaluation, all losses are expressed as an absolute percentage of the total flux.

A. Masking Loss

To evaluate the masking loss, we simulate a headlight at a resolution of 30 000 px × 10 000 px to eliminate sampling losses. It outputs a high beam light distribution with a safety margin-free ideal mask applied just to the vehicle bounding box. For all following evaluations, we simulated a left headlight with a common FOV of 30° × 10° and an opening angle offset towards the left side (see Fig. 9). This matches an actual left headlight and causes a shift of the masking loss towards

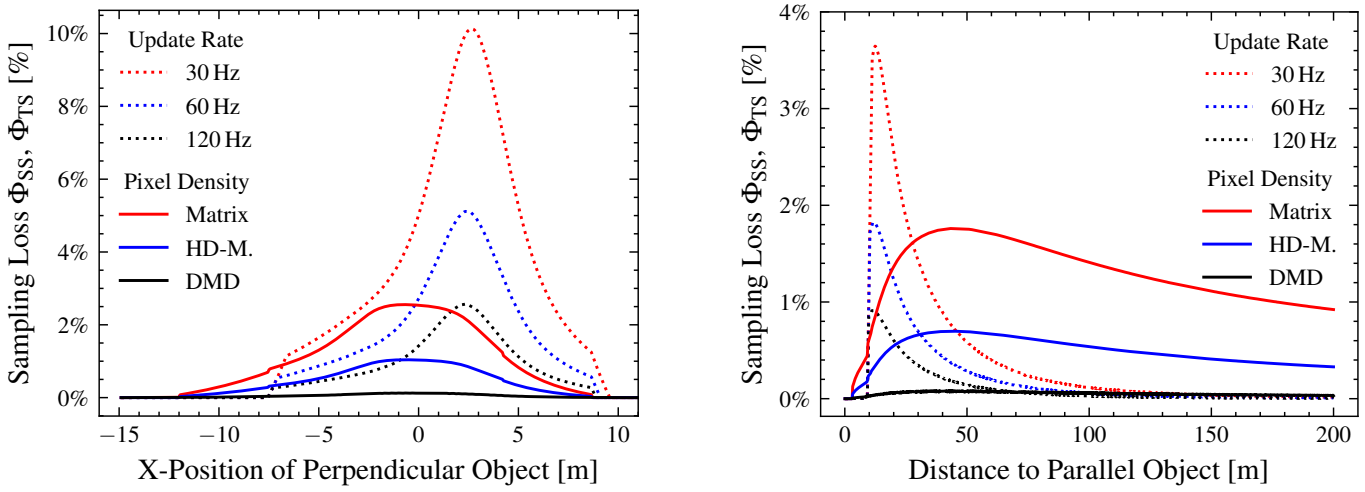

(a) Perpendicular sampling loss

(b) Parallel sampling loss

Fig. 11. The plots show that spatial sampling losses (solid lines) depend on the pixel density of the headlight technology and are negligible for DMD pixel densities. Temporal sampling losses (dotted lines) vary depending on the headlamp update rate and the driving direction of the masked vehicle. In the perpendicular case, the vehicle driving towards the left causes the highest temporal loss at an X-position of 2.5 m, when the safety margin overlaps the hot spot of the high beam distribution.

the left side. For the perpendicular scenario, Fig. 10a shows the loss due to the masking of a vehicle crossing 30 m in front of the headlight. When taking the high beam light distribution into account, a loss of 40 % is visible when the masked vehicle is directly in front of the headlight as the center pixels with the highest flux are blocked. The size of the mask stays constant while the vehicle moves through the illuminated area at a constant distance. In the homogeneous approximation, the luminous flux in the masked area is therefore constant while the bounding box is full within the FOV of the headlight. A maximum of 8 % of the illuminated pixel area is lost. For most positions of the perpendicular scenario, the homogeneous simplification underrates the loss significantly.

In Fig. 10b, the parallel case of opposing vehicles offset by 2 m is shown. As shown in the visualization above the graph, the size of the ideal mask increases for closer distances until the masked vehicle leaves the FOV of the headlight when it is closer than 10 m. The masked vehicle moves on a trajectory through the vanishing point of the headlight. This vanishing point lies directly in front of the vehicle and is very close to the maximum flux of a high beam light distribution. Therefore, in the parallel case, even a small mask has a significant impact on the light throughput. The homogeneous approximation overestimates the parallel masking loss for distances smaller than 10 m as the mask covers almost the entire left side of the FOV, but does not include the center hot spot of the light distribution. At 10 m, it overrates the loss at 34 % compared to the high beam distribution at 24 %. For distances above 10 m, the mask covers a smaller size of bright pixels towards the center, which causes the homogeneous approximation to underestimate the parallel masking loss.

B. Spatial Sampling Loss

In contrast to the ideal headlight with infinitesimal small pixels, a real headlight samples the mask and light distribution to a discrete pixel size. To mask an object, discrete pixels must be disabled. Depending on the pixel density, they cover more area in the image plane than necessary to cover the mask, resulting in additional light loss. The spatial sampling loss is the difference between the ideal masking loss shown in Fig. 10 and the loss of a real headlight with discrete pixels. Fig. 11 shows this spatial sampling loss for different headlights with solid lines. The spatial sampling loss is independent of the framerate of the headlight and only depends on the pixel density relative to the size of the masked object. The very high density of the DMD headlight shows no significant spatial sampling loss in both scenarios. The less-dense LED-matrix technology causes an additional sampling loss of up to 3 % of the total flux in the perpendicular scenario and up to 2 % in the parallel case, while the loss of the HD-matrix lies in between. Spatial sampling loss occurs on all sides of the bounding boxes. The perpendicular loss is therefore zero-centered to the optical axis. Similar to the masking loss modeled in the previous section, the highest loss occurs near the center of the high beam light distribution. The light distribution of the left headlight, modeled here is offset towards the left side. Therefore, sampling losses occur asymmetrically for perpendicular offsets between −12 m and 9 m. This matches the region where masking loss occurs, as sampling loss can only occur when the mask is visible. In the graphs of the parallel scenario, a kink is visible at 10 m where the bounding box crosses the left side of the FOV. For very high distances, the curves converge towards a steady minimum loss. This minimum is determined by the sampling loss of the smallest mask of a single pixel at the vanishing point.

C. Temporal Sampling Loss

The safety margins applied to the masks to compensate for relative object motion cause additional temporal sampling loss. This temporal sampling loss depends on the frame rate

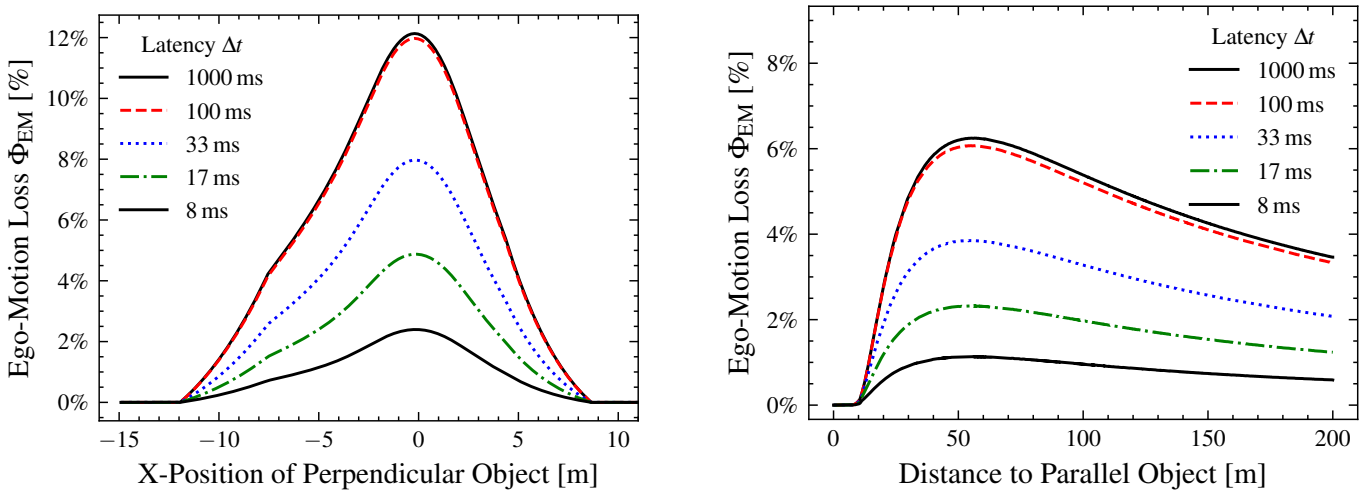

(a) Perpendicular ego-motion loss

(b) Parallel ego-motion loss

Fig. 12. The graphs show the ego-motion loss in both scenarios for different motion-to-photon latencies. Vertical safety margins can compensate for latencies below 100 ms. Above 100 ms, saturation is visible as the safety margin covers the total vertical FOV of the headlight.

of the system but is independent of the pixel density. As described by the model in section IV, higher frame update rates enable smaller safety margins and therefore smaller losses. Fig. 11 shows the temporal sampling loss for the perpendicular scenario at 100 km/h and the parallel scenario at a differential velocity of 200 km/h for headlights with sample rates of 30 Hz to 120 Hz as dotted lines. In the perpendicular scenario, the maximum temporal sampling loss is not centered, but offset in this case by 2 m due to the asymmetric safety margin, which is only applied in the driving direction of the masked vehicle. In this case, the masked vehicle drives to the left, as shown in Fig. 2. Therefore, the safety margin already masks the center region with the highest flux when the vehicle is still 2 m from the optical axis. For a framerate of 30 Hz, this loss is up to 10 % of the total flux. In the parallel case, a safety margin is applied horizontally and vertically in the direction of movement. As the mask stays centered on the vanishing point, the safety margin applied to the outside only includes dimmer parts of the light distribution and therefore only causes a maximum loss of 3.8 % in the 30 Hz case.

D. Ego-Motion Loss

The vertical motion of the ego-vehicle causes a vertical displacement of the virtual screen origin that must be compensated by a vertical safety margin. As explained in section V, this margin depends on the motion-to-photon latency of the system. Fig. 12 shows the additional losses based on our model of the additional vertical safety margins. For latencies above 100 ms, a saturation of the loss is visible in the perpendicular and parallel case. This is earlier than the 200 ms expected by the model shown in Fig. 8 for the safety margin to cover the entire vertical FOV. As the significant part of the total flux is close to the image center, the increase of loss from the tall mask at 100 ms to the full vertical slot at 1000 ms is negligible. Our evaluation shows, that for a compensation of the ego-vehicle movements, a latency below 100 ms is required. Above 100 ms latency, a much simpler vertical slot mask can be used.

VII. Conclusion

The Adaptive driving beam systems of modern headlights apply masks to the projected high beam light distribution to avoid glare for other vehicles on the road. Safety margins extend the masked areas to allow consistent masking of moving objects in dynamic scenarios. We presented a model-based approach to estimate the required size and position of the masks and safety margins for different pixel densities, update rates, and motion-to-photon latencies of the system. We can apply our models to arbitrary driving scenarios with known vehicle trajectories and speeds. We selected the corner cases of perpendicular and parallel driving scenarios relative to the headlight with vehicles traveling at speeds of 100 km/h to evaluate the light throughput of matrix, high-density matrix, and DMD headlights. We provided separate estimates for the flux loss due to masking and the safety margins required to compensate for spatial sampling, temporal sampling, and the ego-motion of the vehicle.

In the simulated scenarios, the vehicle masking caused a reduction of the light throughput of up to 40 %. Our evaluation shows that the mask size alone cannot approximate the masking loss for an actual high beam headlight. Our model based on an actual high beam light distribution shows up to four times higher loss than the homogeneous approximation based on the mask size. High-density matrices enable spatial sampling losses below 1 % of the total light flux in the evaluated perpendicular and parallel traffic scenarios. An update rate of 60 Hz can reduce temporal sampling losses below 5 %. We computed a vertical safety margin based on a suspension model to achieve continuous masking and avoid glare caused by the ego-motion of the own vehicle while reducing additional losses. The motion-to-photon latency of the system must be below 17 ms to reduce losses below 5 %. The mathematical model presented in this paper helps establish design guidelines for the parameters pixel density, update rate, and system latency of the next generation of high-density matrix headlight systems.

REFERENCES

[1] S. Weber, A. Buck, and C. Amann, "Laser light in the bmw i8 design, system integration and test," *ATZ worldwide*, vol. 116, no. 9, pp. 44–49, Aug. 2014.

[2] P. Lehnert, "Disability and discomfort glare under dynamic conditions-the effect of glare stimuli on the human vision," *Proceedings of Pal 2001-Progress in Automobile Lighting*, 2001.

[3] T. Irikura, Y. Toyofuku, and Y. Aoki, "Recovery time of visual acuity after exposure to a glare source," *Lighting Research and Technology*, vol. 31, no. 2, pp. 57–61, Jan. 1999.

[4] K. Zuse, "Fotoelektrisch durch gegenlicht steuerbare beleuchtungsvorrichtung," Germany Patent DE1 190 413B, 1958.

[5] E. N. Mazzae, G. Baldwin, A. Andrella, and L. A. Smith, "Adaptive driving beam headlighting system glare assessment," National Highway Traffic Safety Administration, Tech. Rep., 2015.

[6] N. Artmann, "system integration for high resolution front lighting," in *12th International Symposium on Automotive Lighting-ISAL*, 2017, pp. 233–242.

[7] D. Brunne and F. Kalze, "Outlook on high resolution pixel light," in *12th International Symposium on Automotive Lighting-ISAL*, 2017, pp. 243–251.

[8] N. Pfullmann, A. Thiel, M. Thamm, R. Plöger, G. Kloppenburg, A. Wolf, and R. Lachmayer, "From mechanical adb systems to high resolution headlamps-new opportunities of novel headlight systems," in *12th International Symposium on Automotive Lighting-ISAL*, 2017, pp. 357–365.

[9] K. Kosmas and I. J. Kobbert, "Requirements for dynamic levelling devices to prevent headlamp glare blinding oncoming road users," *83rd GRE*, 2020.

[10] S. G. Grötsch, M. Brink, R. Fiederling, T. Liebetrau, I. Möllers, J. Moisel, H. Oppermann, and A. Pfeuffer, "μafs high resolution adb/afs solution," SAE Technical Paper, Tech. Rep., 2016.

[11] HELLA GmbH, "New headlamp dimension: Liquid crystal hd technology enables fully adaptive light distribution in real time," https://www.hella.com/press/de/Technology-Products-27-06-2017-15695.html, 2017.

[12] V. R. Bhakta and B. Ballard, "High resolution adaptive headlight using texas instruments dlp® technology," in *11th International Symposium on Automotive Lighting-ISAL*, 2015, pp. 483–494.

[13] C. Gut, I. Cristea, and C. Neumann, "High-resolution headlamp," *Advanced Optical Technologies*, vol. 5, no. 2, pp. 109–116, Jan. 2016.

[14] D. Schneider, "Markinglight: Safety enhancement by markinglight systems and their technical implementation," in *6th International Symposium on Automotive Lighting-ISAL*, 2011.

[15] C. Gut, M. Fiege, and B. Böke, "Digital light–experiences with the development of high resolution headlights at daimler," in *12th International Symposium on Automotive Lighting-ISAL*, 2017, p. 253.

[16] M. Maier, J. Moisel, and F. Herold, "Multibeam headlights in the mercedes-benz cls-class," *ATZ worldwide*, vol. 117, no. 2, pp. 4–9, Feb. 2015.

[17] C. Schneider, M. Meyer, and T. Kunz, "Automotive 3d reconstruction based on multi-pixel led headlight systems," in *Fahrerassistenzsysteme 2017*. Springer Fachmedien Wiesbaden, 2017, pp. 85–112.

[18] J. Lee, "Implementation of pixel technology for automotive lighting system based on wafer-level process," in *13th International Symposium on Automotive Lighting-ISAL*, 2019, p. 291.

[19] Y. Takahashi, Y. Kita, and U. M, "Development of 288 segments matrix adb system with improved visibility and safety," in *12th International Symposium on Automotive Lighting-ISAL*, 2017, pp. 323–332.

[20] T. Taki and M. Strassburg, "Review-visible leds: More than efficient light," *ECS Journal of Solid State Science and Technology*, vol. 9, no. 1, p. 015017, 2020.

[21] S. Cladé, "4k pixel solid state glare free high beam," in *13th International Symposium on Automotive Lighting-ISAL*, 2019, p. 269.

[22] OSRAM Opto Semiconductors, "Intelligent forward lighting (fwl) and projection," https://www.osram.com/os/applications/automotive-applications/eviyos-digital-light.jsp, 2021.

[23] T. Wartzek, M. Saure, and C. Wilks, "Digital light - from bulb to interaction," *ATZ worldwide*, vol. 122, no. 11, pp. 40–45, Nov. 2020.

[24] C. J. Reinert-Weiss, H. Baur, S. A. A. Nusayer, D. Duhme, and N. Frühauf, "Development of active matrix lcd for use in high-resolution adaptive headlights, amlcd for high resolution adaptive headlights," *Journal of the Society for Information Display*, vol. 25, no. 2, pp. 90–97, Feb 2017.

[25] W. Huhn, M. Hamm, S. Berlitz, and S. Omerbegovic, "Digital light from matrix to micro mirror," *ATZ worldwide*, vol. 120, no. 2, pp. 18–23, Feb. 2018.

[26] R. Tamburo, E. Nurvitadhi, A. Chugh, M. Chen, A. Rowe, T. Kanade, and S. G. Narasimhan, *Programmable Automotive Headlights*. Springer International Publishing, 2014, vol. 8692, ch. 49, pp. 750–765.

[27] R. Hartley and A. Zisserman, *Multiple View Geometry in Computer Vision*, 2nd ed. Cambridge University Press, Mar. 2004.

[28] S. El Khadri, X. Moreau, A. Benine-Neto, M. Chevrié, W. M. Gonçalves, and F. Guillemard, "Design of the crone automatic headlight leveling system," *IFAC-PapersOnLine*, vol. 55, no. 27, pp. 208–213, 2022.

[29] B. Iribe, "Virtual reality-a new frontier in computing," *AMD Developer Summit APU13*, 2013.

[30] *Adaptive Driving Beam System J3069*, SAE Std., 2021. [Online]. Available: https://www.sae.org/standards/content/j3069_202103

[31] *Regulation No 48 Uniform provisions concerning the approval of vehicles with regard to the installation of lighting and light-signalling devices*, UNECE Std., 2016. [Online]. Available: https://op.europa.eu/en/publication-detail/-/publication/192086c4-870f-11e6-b076-01aa75ed71a1

[32] D. Richardos, B. Anastasia, D. Georgios, and A. Angelos, "Vehicle maneuver-based long-term trajectory prediction at intersection crossings," in *2020 IEEE 3rd Connected and Automated Vehicles Symposium (CAVS)*, 2020, pp. 1–6.

[33] S. Chantranuwathana and H. Peng, "Practical Adaptive Robust Controllers for Active Suspensions," in *ASME International Mechanical Engineering Congress and Exposition*, Nov. 2000, pp. 255–262.

[34] R. N. Jazar, *Quarter Car*. Boston, MA: Springer US, 2008, pp. 931–975.

[35] R. de Charette, R. Tamburo, P. C. Barnum, A. Rowe, T. Kanade, and S. G. Narasimhan, "Fast reactive control for illumination through rain and snow," in *2012 IEEE International Conference on Computational Photography (ICCP)*, 2012, pp. 1–10.

Jens Schleusner received his B.Sc. degree in computer engineering in 2014 and his M.Sc. degree in electrical engineering in 2016 from Leibniz University Hanover, Germany. Since 2017, he has been a research assistant at the Institute of Microelectronic Systems at Leibniz University Hanover, Germany. He is currently researching low-latency rendering algorithms, efficient embedded processing architectures, and applications for high-density matrix headlights for his doctoral studies.

Holger Blume received his Dipl.-Ing. degree in electrical engineering from the University of Dortmund, Germany in 1992. There he also finished his Ph.D. in the nonlinear fault-tolerant interpolation of intermediate images in 1997. From 1998 to 2008 he worked as a senior engineer at the RWTH Aachen University. There he finished his habilitation degree in design space exploration for heterogeneous architectures in 2008. In 2008 he was appointed professor at the Institute of Microelectronic Systems at Leibniz University Hanover. Prof. Blume is chairman of the German chapter of the IEEE Solid-State Circuits Society. His research interests are in design space exploration for algorithms and architectures for biomedical applications and driver assistance systems.

Sebastian Lampe received his B.Eng. degree in media technology from the University of Applied Sciences Emden/Leer, Germany in 2010 and his M.Sc. degree in computational visualistics from the Otto von Guericke University Magdeburg, Germany in 2012. From 2013 to 2018 he worked as a researcher in the field of augmented and virtual reality for the Volkswagen AG Group Innovation. Since 2018, he has been a project manager at the Exterior Lighting System department, Volkswagen AG.